

# An Uncertainty Propagation Architecture for the Localization Problem

Arnaud CLERENTIN, Laurent DELAHOUCHE, Eric BRASSART, Cyril CAUCHOIS  
CREA - Centre de Robotique, d'Electrotechnique et d'Automatique  
IUT, département Informatique, Avenue des Facultés, 80000 Amiens – France  
{Arnaud.Clerentin, Laurent.Delahoche}@u-picardie.fr

## ABSTRACT

In this article, a dynamic localization method based on multi target tracking is presented. The originality of this method is its capability to manage and propagate uncertainties during the localization process. This multi-level uncertainty propagation stage is based on the use of the Dempster-Shafer theory. The perception system we use is composed of an omnidirectional vision system and a panoramic range finder. It enables to treat complementary and redundant data and thus to construct a robust sensorial model which integrates an important number of significant primitives. Based on this model, we treat the problem of maintaining a matching and propagating uncertainties on each matched primitive in order to obtain a global uncertainty about the robot configuration.

**KEYWORDS :** *mobile robot localization, omnidirectional vision, uncertainty management, multi target tracking*

## 1 INTRODUCTION

Localization is a fundamental problem in mobile robotics. Mobile robots have to be able to locate themselves in their environment in order to accomplish their tasks. In order to act in a robust way and to increase the reliability in operation, the robot should consider data as uncertain and all decision should be made using data of an appropriate level of certainty. The localization method presented in this paper has the particularity to integrate uncertainty quantification and to propagate low-level data uncertainties along the localization process. The goal is to obtain a global uncertainty about the robot localization. In this purpose, we propose an architecture which allows to manage and propagate uncertainty. The Dempster-Shafer theory [8] is the key tool of this architecture. Indeed, this formalism enables to easily treat uncertainty since it permits to attribute mass not only on single hypothesis, but also on union of hypothesis. We can thus express ignorance. This is the main difference with Bayesian theory.

Localization methods can be classified as being relative (based on the use of proprioceptive data) or absolute (based on the use of exteroceptive data). Absolute methods consist in determining the robot's position with the only use of exteroceptive data: the robot's configuration is calculated in the environment reference without using previous information [1][5]. But the problem of this kind of localization is linked to the matching stage between the sensorial model and the theoretical map of the environment: this stage can be highly combinative and non robust in

connection with multiple solutions, for example with symmetrical environments. In order to increase the reliability and decrease the computation time of these methods, the use of multi target tracking can be interesting. In the case of the localization problem, multi target tracking can be seen as a propagation of an initial matching. This paradigm is abundantly treated in the literature, for example by Bar Shalom [4]. The methods generally used are probabilistic ones and the two main are JPDAF (Joint Probabilistic Data Association Filter) [4] and MHT (Multiple Hypothesis Tracker) [3]. But these two methods have some drawbacks. They need to know the false alarm rate. The JPDAF takes into account a fixed number of targets and doesn't initialize new tracks. The MHT has combinatorial problems. Therefore, we propose in this paper a multi target tracking method for the localization problem based on the Dempster-Shafer theory used in a framework called *extended open world* [7]. Since this method uses DS theory, it naturally integrates our uncertainty propagation architecture and enables to manage an uncertainty for each target. It allows also to treat the problem of target apparition and momentarily disappearance.

This paper is organized as follow. In a first part, we present our perception system. Then we deal with the target classification stage based on the exploitation of the complementary and redundancy of the data provided by our perception system. Section 4 explains our target tracking algorithm. The paper ends with experimental results presentation.

## 2 THE OMNIDIRECTIONAL PERCEPTION SYSTEM

Our original perception system uses two omnidirectional sensors in cooperation: the omnidirectional vision system SYCLOP and a panoramic range finder system [10] (Fig. 1).

These two sensors have been developed and used independently within our laboratory. The range finder system is an active vision sensor [10]. It allows to obtain a robust omnidirectional range finding sensorial model. The interest of this system is on the one hand its low cost and on the other hand its robustness facing a high incidence angle. The SYCLOP system [2], similar to the COPIS one [14], is composed of a conic mirror and a CCD camera. It enables us to get radial straight lines which characterize angles of every

vertical object such as, for example, doors, corners, edges (Figure 2)...

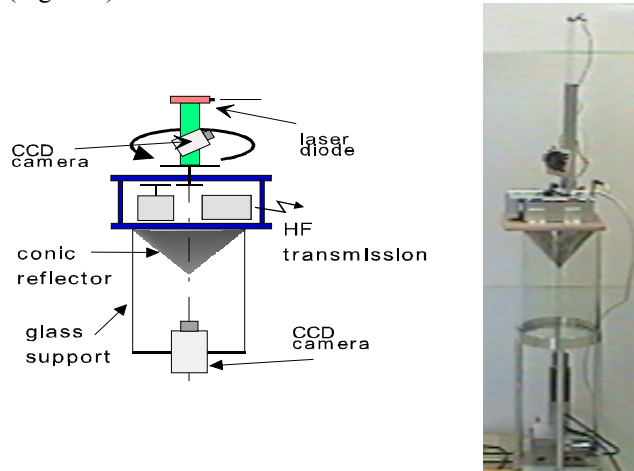


Figure 1: The perception system and the prototype we built.

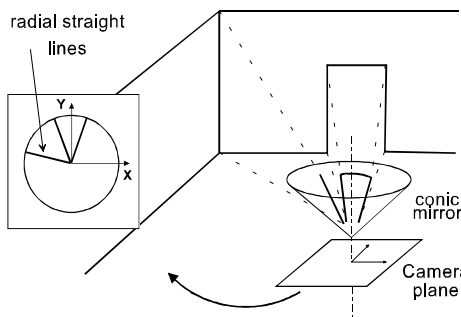


Figure 2: Principle of the omnidirectional sensor SYCLOP

This two omnidirectional sensors association is interesting since it permits to manage some complementary and redundant information within the same sensorial model :

- With SYCLOP, the radial straight lines give the angular position of every vertical object, but the information of depth cannot be achieved in one acquisition: it is not possible to differentiate with this only sensor the notion of opening (corridor, opening of door...) and the notion of vertical object (closed door, radiator,...) (Figure 3).
- The range-finder system, following a segmentation stage [10], permits to exploit sensorial primitives that are segments. In this case we have the notion of depth, but it is impossible to differentiate two vertical objects placed in the same alignment: two closed doors placed on the same wall. It misses the notion of angle that will be provided by the SYCLOP system.

So this association enables to construct a highly descriptive sensorial model, richer than the models obtained with each sensor individually (Figure 3).

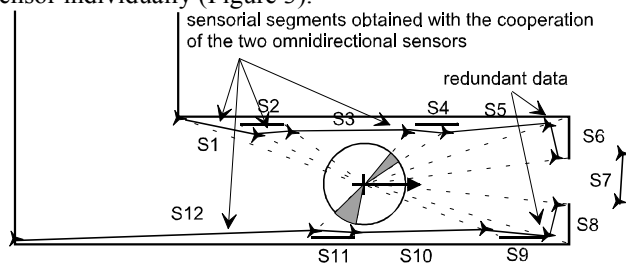


Figure 3: Principle of the omnidirectional sensorial cooperation.

### 3 SENSORIAL MODEL CONSTRUCTION

#### 3.1- Segment primitives determination and associated uncertainty computation

The final primitives of the sensorial model are segments. They are determined with two types of approaches [6]:

- data complementarily approach. The first case concerns the data detected by SYCLOP but not by the depth sensor. In this case, the treatment consists in cutting up segments gotten with the range finder in subsegments according to the radial straight lines of the vision system (case 2 of Figure 4). The second case concerns the data detected by the depth sensor but not by SYCLOP. In this case, the breakpoint gotten by the Duda Hart segmentation method is directly considered (case 3 of Figure 4).
- data redundancy approach. The redundant aspect is characterized by the detection of a vertical landmark with the two sensors (Figure 4). In this case, we use the radial straight line to determine the segment endpoint. Indeed, we consider that the SYCLOP sensor has a better angular precision.

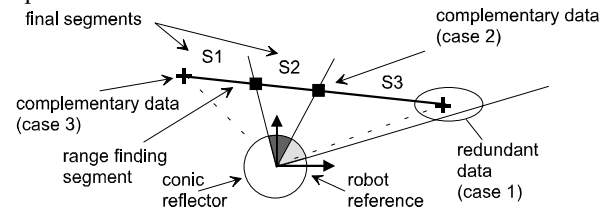


Figure 4: The different cases of the cooperation algorithm.

After the determination of the sensorial model, we compute the reliability, i.e. the uncertainty of each segment. This stage is preponderant for the multi-target tracking stage presented in this article. In this purpose, we take into account five criteria.

The first criteria is the mean distance between the range finding points contained by the segment and this segment. If this mean distance is high, it means that the points are not very well aligned, so this segment is not very sure.

The second criteria is the number of points supported by the segment. This criteria is only discriminative when the segment contains very few points. In this case, it is not very sure.

The third criteria is the segment density of points. As shown in [10], a major drawback of this kind of triangulation depth sensor is a decreasing resolution with an increasing distance. So, this criteria, which is linked to the mean distance between the sensor and the set of point, is a good indicator of the segment reliability (more distant the set of points is, less the precision is).

The fourth criteria analyzes if the segment is detected by one or by the two sensors. The worst case occurs when the two extremities of the segment are detected only by the laser range finder (case 1 of Figure 5). The best case occurs when the two extremities are detected by the two sensors (case 5 of Figure 5). Between these extreme cases, we can distinguish three others cases [6].

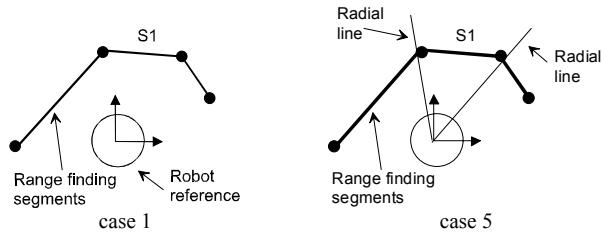


Figure 5 : the two extreme cases of the fourth criteria.

The last criteria concerns a gray level curve extracted from the SYCLOP image. We take into consideration five concentric gray level circles whose average is made. We obtain thus one gray level curve from 0 to 360 degrees. We apply on the portions of curve which represent a segment a least square algorithm. We obtain a straight line and we compute the mean difference of the gray level values from this line. If the difference is high, this means that the gray level sector is not constant. This case occurs generally when a landmark has not been detected by SYCLOP, so this segment is not sure (Figure 6).

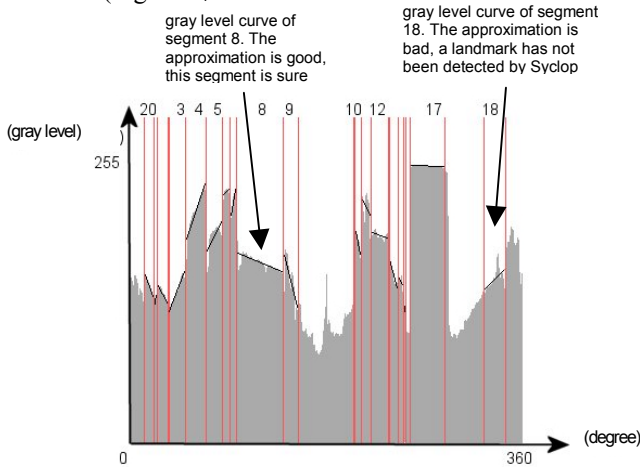


Figure 6: an example of gray level curve concerning the fifth criteria.

The fusion of these five criteria is made thanks to the Dempster-Shafer theory [8]. Our frame of discernment (FOD) is composed of two elements: "YES" and "NO" corresponding to the assertions "The segment exists" and "the segment does not exist". We show on Figure 7 one of the five BPAs which integrates the ignorance quantification. The Dempster rule of combination [8] gives  $m_{seg}(YES)$ ,  $m_{seg}(NO)$  and  $m_{seg}(\Theta)$ . The segment uncertainty is denoted by this set mass  $m_{seg}$ . We have studied on 50 experimental sensed map the conflict between these five criteria. Indeed, these five criteria are redundant and conflict can arise. Experimentally, we have noticed that it is not important (mean conflict = 0.13). This shows that these criteria are pertinent and lead to a consensual decision. But, in certain cases, the conflict is high. So, we have decided to work in an *open world* context [12], i.e. not to normalize. Indeed, in case of high conflict, as Zadeh showed, a normalization can lead to an aberration. On the other hand, a non normalization gives us a precious indication about the conflict between the five criteria. So we report the conflict (the mass on  $\emptyset$ ) to the ignorance  $\Theta$ .

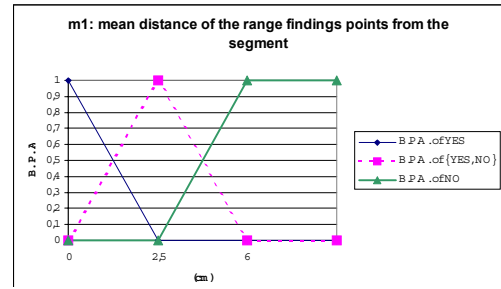


Figure 7: B.P.A of the first classification criterion ( $\{YES, NO\} = \Theta$ )

### 3.2- High level primitives determination

The next stage consists in determining high semantic level primitives which are: "corner", "edges", "wall" and "other" (Figure 8). The "other" class characterizes landmarks which are not "corner", "edges", "wall".

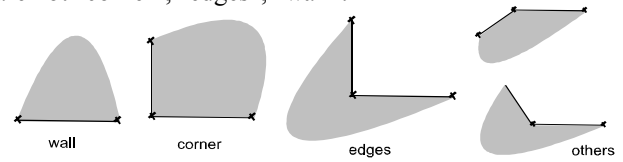


Figure 8: High level semantic primitives.

We use the high semantic level entities "corner", "edge" and "other" because the azimuth angle of the junction of the two segments is a "strong" angle (important existence probability): it is a discriminating angle in connection with the occultation problem. The angles of a segment primitive can be false angle due to occultation.

As in the previous step, we compute an uncertainty linked to each primitive. This uncertainty is determined by propagating the segment(s) uncertainty(ies) computed on the previous step. We reach this aim in two stages. Firstly, we determine the type of the primitive. Secondly, we compute its uncertainty.

We determine the primitive type by fusing two criteria (Figure 9). The first criteria  $m_1$  is the angle  $\alpha$  between two consecutive segments S1 and S2 of the sensorial model. The second criteria  $m_2$  is the minimal distance  $d$  between the "junction" extremities of the two segments S1 and S2. The belief functions of these two criteria are discussed on [9].

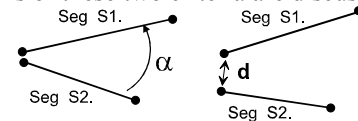


Figure 9: angle criteria and minimal distance criteria.

The fusion is made thanks to the Dempster rule of combination and enables to obtain the mass set  $m_{type}$  by fusing  $m_1$  and  $m_2$ . The two criteria taken into account are complementary, so there is no conflict. The taken decision is the one which has the maximal credibility.

The second stage consists in computing the high level primitive uncertainty. In this purpose, we take into account two uncertainties:

- the uncertainty of the segment(s) composing the primitive
- the uncertainty on the primitive type computed on the first stage.

The FOD is composed of two elements: YES and NO corresponding to the assertions “YES, the primitive exists” and “NO, the primitive does not exist”. The first criteria  $m_{1prim}$  is linked to the segment uncertainty coefficient  $m_{seg}$ .

$$\text{For a primitive wall: } \begin{cases} m_{1prim}(YES) = m_{seg}(YES) \\ m_{1prim}(NO) = m_{seg}(NO) \\ m_{1prim}(\Theta) = m_{seg}(\Theta) \end{cases}$$

For a primitive corner, edge or other composed of two segments S1 et S2:

$$\begin{cases} m_{1prim}(YES) = m_{seg}^{S1}(YES) \oplus m_{seg}^{S2}(YES) \\ m_{1prim}(NO) = m_{seg}^{S1}(NO) \oplus m_{seg}^{S2}(NO) \\ m_{1prim}(\Theta) = m_{seg}^{S1}(\Theta) \oplus m_{seg}^{S2}(\Theta) \end{cases}$$

The second criteria  $m_{2prim}$  for a primitive of type  $T$  is computed according to the following rules:

$$\begin{cases} m_{2prim}(YES) = Cr(T) \\ m_{2prim}(NO) = \sum_{A \in \Theta, A \cap T = \emptyset} m_{type}(A) = Cr(\bar{T}) \\ m_{2prim}(\Theta) = \sum_{A \in \Theta, A \neq T, A \cap T \neq \emptyset} m_{type}(A) = Pl(T) - Cr(T) \end{cases}$$

The mass for the YES is equal to the belief we have on  $T$ , i.e. the credibility of  $T$   $Cr(T)$ . The mass for the NO is equal to the disbelief on  $T$ , i.e. the mass which is not on  $T$ . The mass for  $\Theta$  represents the uncertainty about  $T$ , i.e. the mass which is on focal elements which include  $T$ . Doing this, we respect the constraint that the mass sum must be equal to 1.

By fusing the two criteria  $m_{1prim}$  et  $m_{2prim}$ , we obtain the uncertainty of the primitive through  $m_{prim}(YES)$ ,  $m_{prim}(NO)$  and  $m_{prim}(\Theta)$ . Doing this, we estimate the uncertainty of the high level primitives by propagation of the segments uncertainty.

So, at the end of this step, we have four lists of primitives (a list of corners, of edges, etc.) with an associated uncertainty for each primitive through the set mass  $m_{prim}$ . This uncertainty includes the uncertainty about the type of the primitive and the uncertainty about the existence (the reliability) of the segments which compose the primitive.

## 4 DYNAMIC LOCALIZATION METHOD

### 4.1 - Algorithm

Our localization method is based on a tracking of high semantic level primitives: we propagate the matching made at an acquisition  $n$  on an acquisition  $n+1$ . So, the problem to solve is the following: propagation of an initial matching on the acquisitions realized during the robot’s displacement. The initial matching is done in manual way or with the absolute localization method presented in [6]. Then we try to pursue the matching. To confirm a matching propagation, we must before generate a prediction which will be compared to the observations. So we have developed a prediction system based on a linear extrapolation of the azimuth angle curves of the high level primitives (on experimental results, we can note that the angles variation is locally linear): we generate a predictive observation vector composed of angles got by linear extrapolation (Figure 11). For example, if we examine

the evolution of the landmark angles  $\Theta_1$ ,  $\Theta_2$  and  $\Theta_3$  (Figure 10), we remark that the curve can be extrapolated in order to have a prediction  $\Theta_{4p}$ . If a matching is done between  $\Theta_{4p}$  and an angle observation, the track is propagated.

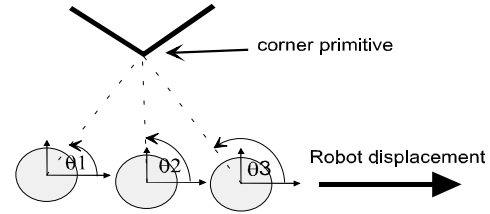


Figure 10: evolution of landmark angles.

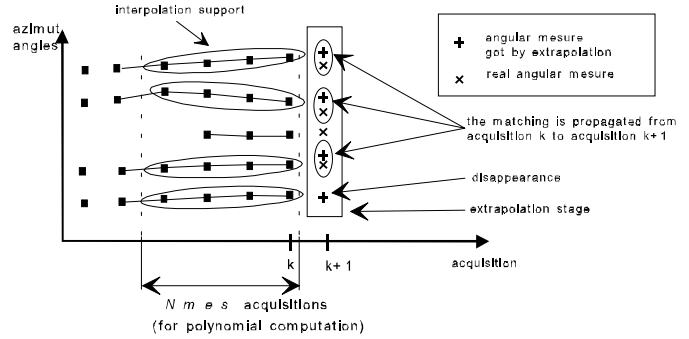


Figure 11: principle of angular measures extrapolation.

Our prediction heuristic is robust since it is based on angle curves of high level primitives: the extrapolated measures correspond to “strong” angles whose evolution curves can not confuse themselves because they do not suffer of occultation phenomena.

At this level, the problem is to match for each type of primitive the  $p$  angular observations obtained at the acquisition  $t$  with the  $q$  predictions. These  $q$  predictions are computed from the  $Nmes$  last observations. To reach this aim, we use the Dempster-Shafer theory in the framework of *extended open word* [7] because of the introduction in the FOD of an element noted  $*$  which represents all the hypothesis which are not modeled.

For each prediction  $Q_j$  ( $j \in [1, q]$ ), we apply the following algorithm.

- The frame of discernment  $\Theta$  is composed of:
  - the  $p$  observations ( $P_i$  means “the prediction  $Q_j$  is matched with the observation  $P_i$ ”)
  - and the element  $*$  which means “the prediction  $Q_j$  cannot be matched with one of the  $p$  observations”.

$$\text{So: } \Theta = \{P_1, P_2, \dots, P_p, *\}$$

- The matching criterion is the angular difference between observation  $P_i$  and prediction  $Q_j$  (Figure 11).
- For each observation  $P_i$ , we compute :
  - $m_i(P_i)$  the mass associated with the proposition “ $P_i$  is matched with  $Q_j$ ”.
  - $m_i(\bar{P}_i)$  the mass associated with the proposition “ $P_i$  is not matched with  $Q_j$ ”.
  - $m_i(\Theta_i)$  the mass represented the ignorance concerning the observation  $P_i$ .

The BPAs are shown on Figure 12.

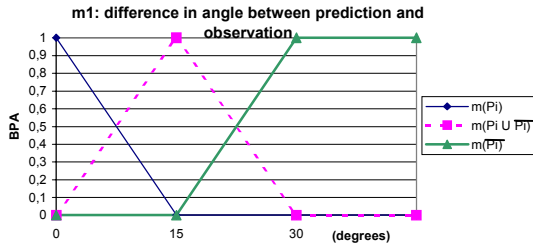


Figure 12: BPA of the matching criterion.

After the treatment of all the  $P_i$  observations, we have  $p$  triplets :

$m_1(P_1)$	$m_1(\bar{P}_1)$	$m_1(\Theta_1)$
$m_2(P_2)$	$m_2(\bar{P}_2)$	$m_2(\Theta_2)$
...	...	...
$m_p(P_p)$	$m_p(\bar{P}_p)$	$m_p(\Theta_p)$

We fuse these triplets and we get  $m_{match}(P_1)$ ,  $m_{match}(P_2)$ , ...,  $m_{match}(P_p)$ ,  $m_{match}(\Theta)$  and  $m_{match}(\Theta)$  by using the condensed formulas obtained by Gruyer in [11].

- The final decision is the one which has the maximal BPA.
- Experimentally we can note that ambiguities can appear after this step, but only on the segment primitives: a segment observation  $P_i$  can be matched with two segment predictions  $Q_i$ , this case is impossible in the reality. So we use, like Gruyer, only for this class of primitives, a traditional assignment Hungarian algorithm to match one observation with one prediction [11].

Finally, this matching method enables us to easily manage primitive appearances and disappearances:

- If an element  $P_i$  of the FOD cannot be matched,  $P_i$  is an appeared primitive and a track can be initialized.
- If a prediction  $Q_j$  is matched with \*, the track is temporarily or definitively lost.

#### 4.2 - Management of an appearance

From the position computed with the matched primitives, we try to match the appeared primitives with the primitives of the theoretical map which is composed of four lists (a list of wall, a list of corner, etc.). In other words, we try to initiate a new track. We have to distinguish two cases: primitives wall and the other primitives.

For each appeared primitive wall, we have considered three correspondence tests applied on all the theoretical wall primitives [13] :

- angular difference  $\alpha$  between the two segments,
- difference in length ( $L_s - L_m$ ) between the two segments,
- distance  $D$  between the centers of the two segments.

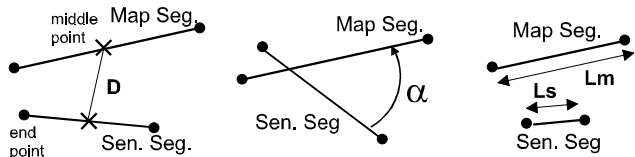


Figure 13: The three matching criteria.

The fusion of these three treatments is made thanks to the Dempster-Shafer theory. Our FOD is composed of two elements: YES and NO corresponding to those assertions : "Yes, we can match the two walls" and "No, we can not

match the two walls". For each criterion, we have determined the BPAs  $m_1$ ,  $m_2$ ,  $m_3$  (see Figure 14 for an example of BPA).

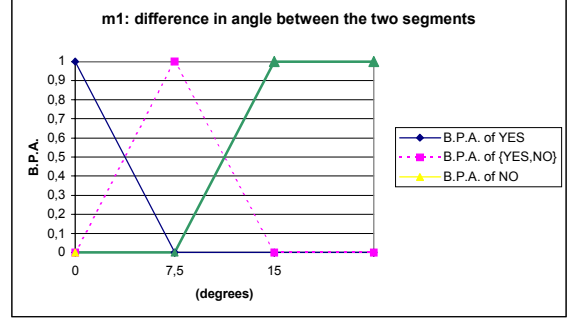


Figure 14: :basic probability assignments of the first matching criteria ( $\{YES, NO\} = \Theta$ )

We can then perform the combination calculation thanks to the Dempster-Shafer rules without renormalization [12] in order to get a mass set  $m_m$ . The non-renormalization gives us a precious indication about the conflict. Generally, we have experimentally noticed that this conflict is null, but, in a few cases, it can be high. This occurs for example when we examine two parallel walls. So, if the conflict  $k$  is superior to 0.7, we think this value is too high and we take a prudent decision: we don't match the two segments. If  $k < 0.7$ , we can take a decision and the segments are matched if BPA for the YES  $m_m(YES)$  is superior to the BPA for the NO  $m_m(NO)$ .

For each other primitive (corner, edge, other), we consider two correspondence tests (Figure 15):

- The difference between the robot-sensorial primitive distance  $d_{seg}$  and the robot-map primitive distance  $d_{map}$ .
- The difference between the sensed primitives angle  $\Theta_{seg}$  and the theoretical primitive angle  $\Theta_{map}$ .

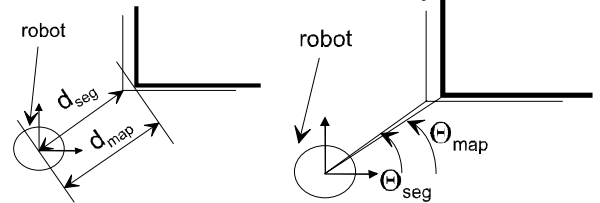


Figure 15: The two matching criteria

As the previous case, our FOD is composed of two elements: YES and NO. The fusion is realized according to the same strategy as the wall primitives.

#### 4.3 - Management of a disappearance

As we will see in paragraph 4.4, if a matching is not propagated, the track is not immediately cancelled but its uncertainty increases. If this uncertainty becomes too high, we definitively cancel this track.

#### 4.4 - Track uncertainty management

For each track, we manage an associated uncertainty with the help of the Dempster-Shafer theory. Our FOD for each track is composed of two elements: "YES" and "NO" which mean "Yes, the track exists" and "No, the track does not exist". Two stages are managed:

**Uncertainty initialization stage.** In the case of a primitive appearance, the initial uncertainty  $m_{track\ 0}$  at time 0 takes into account the uncertainty of the primitive  $m_{prim}$  (paragraph 3.2) and the uncertainty of the first matching  $m_m$  (paragraph 4.2).

So, the two criteria are:

$$\square \begin{cases} m_1(YES) = m_{prim}(YES) \\ m_1(NO) = m_{prim}(NO) \\ m_1(\Theta) = m_{prim}(\Theta) \end{cases}$$

$m_1$  takes into account the uncertainty of the primitive.

□  $m_2$  which takes into account the uncertainty of the first matching through  $m_m(YES)$  [9].

We have noticed on experimental results that conflict can appear, but it occurs in only one case: a good matching of an unreliable primitive. Our strategy to manage this conflict is to reduce the weight of the primitive uncertainty  $m_1$  by an operation of discounting [8]:

$$\text{if } m_1(YES) > 0 : \begin{cases} m_1^\alpha(YES) = m_1(YES) \times (1 - m_1(NO)) \\ m_1^\alpha(NO) = m_1(NO) \times (1 - m_1(NO)) \\ m_1^\alpha(\Theta) = 1 - m_1^\alpha(YES) - m_1^\alpha(NO) \end{cases}$$

We obtain  $m_{track\ 0}(YES)$ ,  $m_{track\ 0}(NO)$  and  $m_{track\ 0}(\Theta)$  by merging  $m_1^\alpha$  and  $m_2$  using the Dempster combination rule.

If  $m_{track\ 0}(NO) > m_{track\ 0}(YES)$ , then we consider that the uncertainty is too high and we don't initialize the track. This taking into account of the primitive uncertainty enables us not to work with all the primitives, we privilege the "robust" and reliable primitives.

**Uncertainty propagation stage.** Then, if the matching can be propagated, the track uncertainty is updated by taking into account:

- In relation with time  $t-1$ : the track uncertainty at time  $t-1$
- In relation with time  $t$ : the primitive uncertainty and the matching uncertainty at time  $t$ .

Let be  $m_{track\ t-1}$  the mass set of the track at time  $t-1$ . The three set masses  $m_1$ ,  $m_2$  and  $m_3$  concerning the 3 criteria are:

- $\begin{cases} m_1(YES) = m_{prim}(YES) \\ m_1(NO) = m_{prim}(NO) \\ m_1(\Theta) = m_{prim}(\Theta) \end{cases}$   $m_1$  takes into account the primitive uncertainty at time  $t$ .
- $m_2$  takes into account the uncertainty of the matching at time  $t$   $m_{match}$  computed on paragraph 4.1 [9].
- $\begin{cases} m_3(YES) = m_{track\ t-1}(YES) \\ m_3(NO) = m_{track\ t-1}(NO) \\ m_3(\Theta) = m_{track\ t-1}(\Theta) \end{cases}$   $m_3$  takes into account the track uncertainty at time  $t-1$ .

We adopt the strategy described in the uncertainty initialization stage: a high conflict only appears when we realize a good matching of an unreliable primitive and we discount the mass of the primitive uncertainty.

$m_{track\ t}(YES)$ ,  $m_{track\ t}(NO)$  and  $m_{track\ t}(\Theta)$  are obtained by fusing  $m_1$ ,  $m_2$  and  $m_3$ .

If the matching is not propagated, the uncertainty of the track increases. In this case, we fix the BPA  $m_{match}$  as follow:

$$\begin{cases} m_{match}(YES) = 0 \\ m_{match}(NO) = 0.2 \\ m_{match}(\Theta) = 0.8 \end{cases}$$

This mass set has been determined experimentally in order to obtain a regular increase of the track uncertainty. So, if  $m_{track\ t-1}$  is the BPAs of the track at time  $t-1$ , we update the uncertainty  $m_{track\ t}$  using the Dempster rule of combination with  $m_{track\ t-1}$  and  $m_{match}$ .

If  $m_{track\ t}(NO) > m_{track\ t}(YES)$ , then we consider that the track uncertainty is too high and the track is definitively lost. Here again, the taking into account of the primitive uncertainty enables us to privilege the tracks with reliable primitives.

**Transition between a primitive wall and an other primitive.** We manage in our system the transition between the primitives corner, edge, other and the primitives wall. An example of such transition is shown on Figure 16. At time  $t$ , the robot detects one of the two faces of the edge and this face is classified as a wall primitive. At time  $t+1$ , the two edge faces are visible from the robot and it detects an edge primitive. The wall detected at time  $t$  and the edge detected at time  $t+1$  correspond to the same track. So we use the uncertainty of the wall track at time  $t$  to initiate the uncertainty of the edge track at time  $t+1$ .

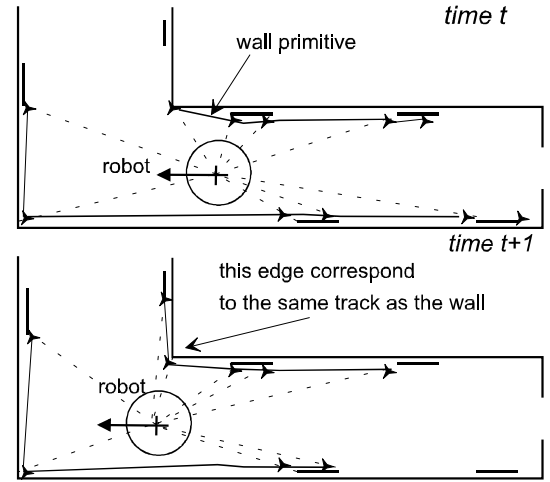


Figure 16: an example of transition wall  $\rightarrow$  edge

#### 4.5 - Localization uncertainty

The last step of our uncertainty propagation architecture is to compute the uncertainty of the robot localization. This aim is reached with the help of the Dempster Shafer theory and the FOD is composed of the two elements YES and NO corresponding to the assertions "Yes, the localization is correct" and "No, the localization is not correct". We take into account  $p+2$  criteria.

The first criterion is the number of high level primitives used to localize the robot. Indeed, if we use few primitives, the localization is not reliable.

The second criterion is a ratio concerning the number of detected primitives and the number of matched primitives. Indeed, if we detect a lot of primitives but if we match only a little few primitives, this can mean that a problem occurs in the classification process or in the matching process. So the localization may be unreliable.

$$\text{ratio} = \frac{\text{number of matched primitives}}{\text{number of detected primitives}}$$

The last  $p$  criteria are the uncertainty of the  $p$  tracks managed by the robot, i.e. the  $p$  mass sets  $m_{track\ t}$  computed in

the paragraph 4.4. If the tracks are uncertain, the localization will be uncertain. Since we merge an important number of mass sets and since the Dempster operator is not idempotent, we apply an operation of discounting on the  $p$  mass sets  $m_{track_t}$ . The discounting coefficient is different if the mass set  $m_{track_t}$  concerns a wall primitive or an other primitive (corner, edge and other): we privilege in the fusion process the “strong” primitives corner, edge and other.

These  $p+2$  criteria are fused according to the Dempster rule and we obtain a mass set  $m_t$  which quantifies the localization uncertainty. This uncertainty is directly issued of the uncertainties of the low-level data which have been propagated, as shown on Figure 17.

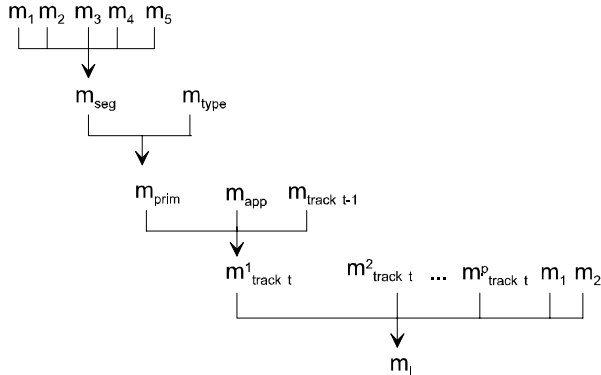


Figure 17 : Uncertainties propagation during the localization process.

## 5 EXPERIMENTAL RESULTS

We have tested our algorithm on several acquisitions made in an indoor environment (the end of a corridor shown Figure 18 whose theoretical map in possession of the robot is on Figure 19). The omnidirectional acquisitions and the localization algorithm are computed in a Pentium PC located on our mobile robot.

On Figure 18, we show an example of high level primitives sensed map. We report on Table 1 the different masses about the primitives uncertainty.

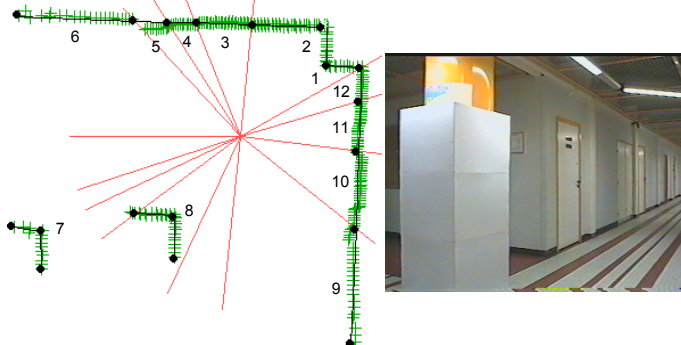


Figure 18: high level primitive map and the real environment.

On a two paths made in the corridor by our robot mobile SARAH, we can note on 42 acquisitions made every 30 cm that the robot’s position is determined correctly with a good precision: the mean error is equal to 13 cm in position and 3 degrees in orientation (Figure 19).

On Figure 18, we represent only the tracked landmarks of the second trajectory. We can remark that our tracking is robust and efficient: among all the important number sensorial primitives, the tracked primitives are correctly

identified and the tracks are generally never lost until the landmarks become invisible from the robot. We show on Figure 21 the uncertainty evolution of edge 6. The initial matching is done manually and the mass set is set as follow:  $m_{track_0}(YES) = m_{track_0}(\Theta) = 0.5$ ,  $m_{track_0}(NO) = 0$ . The landmark is tracked until acquisition 7, so the BPA for YES  $m_{track_t}(YES)$  increases. Then, it becomes invisible from the robot. So the BPA for YES decreases until acquisition 12 where the BPA for NO is superior to the BPA for YES. So the track is definitively lost.

Primitive number	Type	$m(YES)$	$m(NO)$	$m(\theta)$
1	Edge	0.72	0.08	0.20
2	Corner	0.64	0.16	0.20
3	Wall	0.64	0	0.36
4	Wall	0.91	0	0.09
5	Wall	0.07	0	0.93
6	Wall	0.83	0	0.17
7	Edge	0.33	0.25	0.42
8	Edge	0.70	0.03	0.27
9	Wall	0.50	0	0.50
10	Wall	0.11	0	0.89
11	Wall	0.47	0	0.45
12	Corner	0.78	0.03	0.18

Table 1: uncertainties of the primitive model.

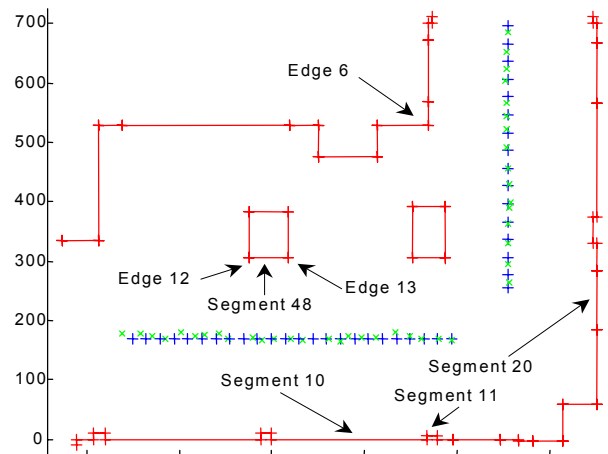


Figure 19: theoretical map and localization results ('+'=real position, 'x'=computed position).

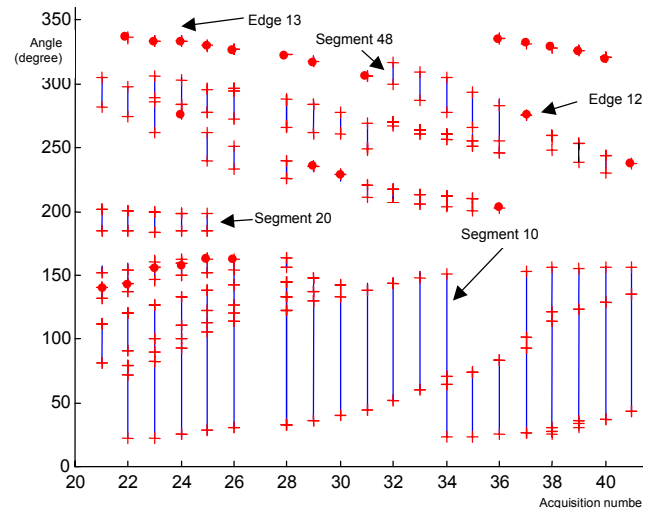


Figure 20: the tracked landmarks ('+'=corner,point=edge, segment=wall)

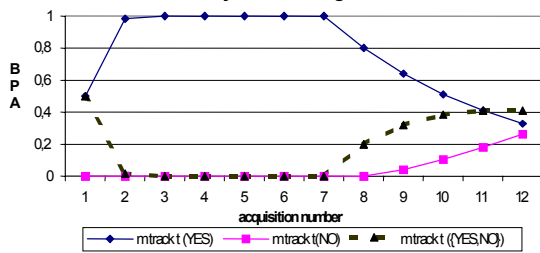


Figure 21: uncertainty evolution of landmark edge 6.

Finally, we see on Figure 16 an example of a double transition edge-segment-edge. Until acquisition 32, the two faces of the edge are visible. On acquisition 33, one face is visible, so a primitive segment is detected but we don't initiate a new track since this segment belong to the edge previously tracked. On acquisition 37, the robot can detect a new edge (edge 12 on Figure 19) that contains the segment. As the previous case, we don't initiate a new track but we prolong the current track.

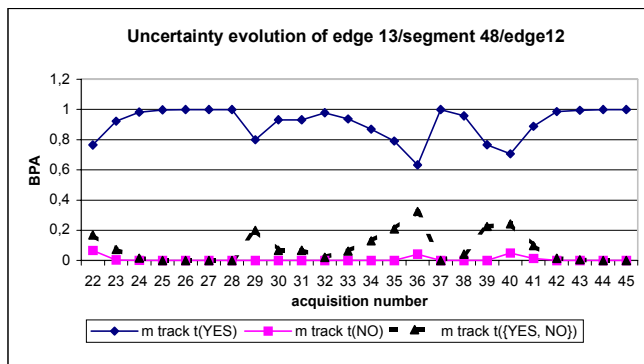


Figure 22: uncertainty evolution of edge 13/segment 48/edge 12.

On Figure 23, we show the evolution of the localization uncertainty. The uncertainties of the first acquisitions are weak : the number of tracked primitives is high. Then this number decreases, so the uncertainty increases, i.e.  $m_t(\text{YES})$  decreases. After acquisition 46, several new tracks are initialized and the uncertainty becomes weak.

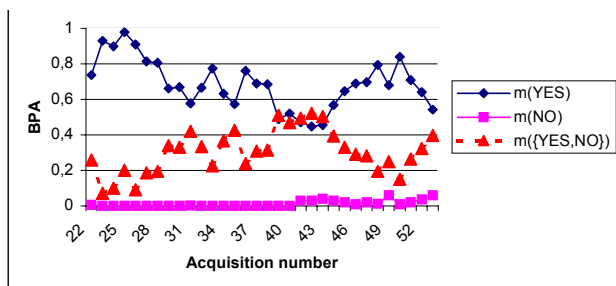


Figure 23 : localization uncertainty.

## 6 CONCLUSION

In this paper, we have studied and implemented a multi level uncertainty propagation architecture. After a multi criteria fusion stage based on the use of the Dempster-Shafer theory, we obtain a multi-valued sensorial map which permits to quantify the credibility of the high level primitives. These

primitives are then used in our dynamic localization method based on a propagation of an initial matching. This method solves two problems linked to the multi target tracking: the propagation of an uncertainty concerning the landmark tracks and the treatment of the apparition and momentary disappearance of a track. This multi-target tracking paradigm has been tested on several robot's path in a large structured indoor environment and has provided good results concerning the matching maintaining and the preciseness of the localization. An extension of this work could concern the linear angular prediction which is mono criteria. A prediction based on a dynamic model or combining 'proprioceptive' could be used and would allow the system to operate on fast moving vehicles.

## 7 REFERENCES

- [1] S. Thrun, "Finding Landmarks for Mobile Robot Navigation", *IEEE Int. Conf. on Robotics and Automation*, May 1998, pp. 958-963.
- [2] L. Delahoche, B. Marhic, C. Pégard, P. Vasseur - "A navigation system based on an omnidirectional vision sensor", *Proc. of Int. Conf. on Intelligent Robots and Systems*, France, Sept. 1997.
- [3] D.B. Reid, "An algorithm for tracking multiple target", *IEEE trans. on automatic control*, vol. AC24, n. 6, pp. 843-844, Dec. 89
- [4] Y. Bar-Shalom, « *Multitarget-Multisensor tracking : Applications and Advances vol.II.* », Artech House, 1992.
- [5] H.R. Beom, H.S. Cho, "Mobile robot localization using a single rotating sonar and two passive cylindrical beacons", *Robotica*, Vol. 13, pp. 243-252, 1995.
- [6] A. Clémentin, L. Delahoche, E. Brassart, "A multi sensor cooperative approach for the mobile robot localization problem", *Proc. of the workshop Performance metrics for Intelligent Systems*. PERMIS2000, Washington, Aug 00
- [7] C. Royère, D. Gruyer, V. Cherfaoui, « Data association with believe theory », *3rd int. conf. on information fusion FUSION 2000*, Paris, France, 2000
- [8] G.A. Shafer, "A mathematical theory of evidence", Princeton : university press, 1976.
- [9] A. Clémentin, L. Delahoche, E. Brassart "Omnidirectional sensors cooperation for multi-target tracking", *IEEE Int. Conf. on Multisensor Fusion and Integration MFI 2001*, Aug. 01, Germany, pp. 335-340
- [10] A. Clémentin, C. Pégard, C. Drocourt "Environment exploration using an active vision sensor", *Proc. IEEE Int. Conf. on Intelligent Robots and Systems (IROS'99)*, Korea, Oct. 1999.
- [11] D. Gruyer, V. Berge-Cherfaoui, "Matching and decision for vehicle tracking in road situation", *Proc. IEEE Int. Conf. on Intelligent Robots and Systems (IROS'99)*, Korea, Oct. 1999.
- [12] Smets Ph., « The nature of the unnormalized beliefs encountered in the transferable belief model », *Proceedings of the 8th Conference on Uncertainty in Artificial Intelligence*, San Mateo, Californie, (1992) 292-297
- [13] Crowley J., « Navigation for an intelligent mobile robot » - *IEEE Journal on Robotics and Automation*, Vol. RA-1, n°1, pp. 31-41, March 1985
- [14] Y. Yagi, Y. Nishizawa, M. Yachida, "Map-based navigation for a mobile robot with omnidirectional image sensor COPIS", *IEEE Trans. on Rob. and Aut.* Vol 11, pp. 634-648, Oct. 1995.